Talanta 109 (2013) 167–172

Contents lists available at SciVerse ScienceDirect

Talanta

journal homepage: www.elsevier.com/locate/talanta

Electrochemistry of cholesterol biosensor based on a novel Pt–Pd bimetallic nanoparticle decorated graphene catalyst

Shurui Cao [a,b], Lei Zhang [b], Yaqin Chai [a], Ruo Yuan [a,]*

[a] *Education Ministry Key Laboratory on Luminescence and Real-Time Analysis, College of Chemistry and Chemical Engineering, Southwest University, Chongqing 400715, China*
[b] *Chongqing Entry Exit Inspection and Quarantine Bureau, Chongqing 400020, China*

ARTICLE INFO

Article history:
Received 17 October 2012
Received in revised form
30 January 2013
Accepted 1 February 2013
Available online 18 February 2013

Keywords:
Cholesterol biosensor
Graphene sheets (GS)
Pt–Pd
Cholesterol oxidase (ChOx)
Hybrid nanocomposites
Direct electrochemistry

ABSTRACT

A new electrochemical biosensor with enhanced sensitivity was developed for detection of cholesterol by using platinum–palladium–chitosan–graphene hybrid nanocomposites (PtPd–CS–GS) functionalized glassy carbon electrode (GCE). An electrodeposition method was applied to form PtPd nanoparticles-doped chitosan–graphene hybrid nanocomposites (PtPd–CS–GS), which were characterized by scanning electron microscopy (SEM) and electrochemical methods. The presence of the PtPd–CS–GS nanocomposites not only accelerated direct electron transfer from the redox enzyme to the electrode surface, but also enhanced the immobilized amount of cholesterol oxidase (ChOx). Under optimal conditions, the fabricated biosensor exhibited wide linear ranges of responses to cholesterol in the concentration ranges of 2.2×10^{-6} to 5.2×10^{-4} M, the limit of detection was 0.75 μM (S/N=3). The response time was less than 7 s and the Michaelis–Menten constant (K_m^{app}) was found as 0.11 mM. In addition, the biosensor also exhibited excellent reproducibility and stability. Along with these attractive features, the biosensor also displayed very high specificity to cholesterol with complete elimination of interference from UA, AA, and glucose.

1. Introduction

Direct electrochemistry of redox enzymes not only provides a model for the study of electron transport of enzymes in biological systems, which is important to understand the material metabolism and energy transformation in life processes, but also achieves direct electron exchange between redox enzymes and electrodes, establishes a foundation for the fabrication of third generation of electrochemical biosensors [1–3]. In a direct electrochemistry-based biosensor, enzymes are integrated with electrodes, the direct electron transfer (DET) of enzymes on an electrode is generally difficult since the enzyme active sites are deeply buried in the protein matrix. To achieve DET, efforts have been devoted to shortening the electron transfer distance and designing biocompatible matrix to retain the native structure of the redox enzymes [4,5]. Nanomaterials are suitable for acting as “electronic wires” to shorten the electron transfer distance, enhance the electron transfer between redox centers of the enzyme and the electrode surface and simultaneously retain the biological activity of the redox enzymes [6]. Graphene-based hybrid nanomaterials are good examples, which could provide larger electrochemically active surface areas for the adsorption of enzymes and effectively accelerate the electron transfer between electrode and detection molecules [7]. Zeng and his colleague successfully synthesized palladium nanoparticle/chitosan-grafted graphene nanocomposites for construction of a glucose biosensor [8]. The hybrid nanocomposites showed a significant increase of electronic conductivity. Dong group successfully synthesized graphene/platinum hybrid nanostructures by alternatively assembling the ionic liquid-modified grapheme nanosheets and platinum nanoparticles [9]. The obtained hybrid nanomaterials exhibited good electrochemical properties. Our group demonstrated a facile strategy to incorporate high-quality hollow CoPt bimetal alloy nanoparticles onto reduced graphene oxide sheet [10]. The formed conjugates provided large surface area for loading plentiful redox probe thionine and showed a significant increase of electronic conductivity. These hybrid nanomaterials displayed superior electrochemical performance in comparison with that of alone nanomaterial. In this work, we tried to fabricate platinum (Pt) and palladium (Pd) nanoparticles-doped graphene hybrid nanomaterials for the preparation of the electrochemical cholesterol biosensor. Due to the unique catalytic activity and chemical selectivity of the bimetallic nanoparticles [11,12], the PtPd nanoparticles-doped grapheme hybrid nanomaterials were found to play the dual roles of catalyzing cholesterol redox reactions and also assisting direct electron transfer from the redox enzyme to the electrode surface.

Chitosan (CS) is a biocompatible polymer. It has been widely used as an immobilization matrix for biofabrication due to its high permeability towards water, excellent membrane forming

---

* Corresponding author. Tel.: +86 23 68252277; fax: +86 23 68254000.
E-mail address: yuanruo@swu.edu.cn (R. Yuan).

0039-9140/$ - see front matter © 2013 Elsevier B.V. All rights reserved.
http://dx.doi.org/10.1016/j.talanta.2013.02.002

ability, good adhesion and biocompatibility [13]. Many literatures also reported that CS can accumulate metal ions through various mechanisms, such as chelation, electrostatic attraction, and ion exchange, depending on the nature of the metal ion and pH of the solution [14,15]. So in this study, chitosan was joined into the dispersed graphene nanosheets (GS) to form homogeneous GS–CS solution. Herein, chitosan not only acts as an effective solubilizing agent for dispersing graphene nanosheets (GS–CS), which can have a good film-forming, but also as a polymer for accumulating Pt Pd ions to obtain a nanostructural graphene–chitosan–Pt–Pd composite membrane with the further enhancement of the porosity, surface area and electronic transfer rate.

In view of the advantageous features of Pt–Pd nanoparticles-doped graphene hybrid nanomaterials and GS–CS composite membrane, a sensitive electrochemical biosensor was constructed using cholesterol as the model analyte. The aim of this study is to design an enzyme sensing biosensor to study the direct electrochemistry of cholesterol oxidase (ChOx) and biosensing for cholesterol. Based on the PtPd nanoparticles-doped chitosan–graphene hybrid nanocomposites (PtPd–CS–GS), direct electron transfer from the redox enzyme to the electrode surface could be achieved by efficient catalysis of the ChOx towards the electrochemical reduction of cholesterol, resulting in the low detection limit of cholesterol. The details of the attractive response performances of the proposed biosensor and potential merits for protein detection are substantiated as follows.

2. Experimental

2.1. Reagents and materials

Graphene sheets (GS) were obtained in Pioneer Nanotechnology Co. (Nanjing, China). Cholesterol oxidase (ChOx, EC 1.1.3.6, ≥ 50 units/mg, from Brevibacterium sp.), Cholesterol ($C_{27}H_{46}O$, Mr: 386.67, $\geq 99\%$ purity, from lanolin), Chitosan (CS), Triton X-100 ($C_{34}H_{62}O_{11}$, MW: 646.85), poly (diallyldimethylammonium chloride) (PDDA, 20% aqueous solution), $PdCl_2$, $HAuCl_4$, H_2PtCl_6 were obtained from Sigma Chemical Co. (St. Louis, MO, USA). Phosphate buffered solutions (PBS) (pH 7.0) were prepared using 0.1 M Na_2HPO_4, 0.1 M KH_2PO_4, 0.1 M KCl and kept at 4 °C before use. The stock solution was prepared by dissolving cholesterol in the mixture of 2-propanol and Triton X-100, and then diluted it only with Triton X-100 solution for preparing standard solutions. Distilled water was used throughout this study. All other chemicals were of analytical grade and used as received without further purification.

2.2. Apparatus

The cyclic voltammetric (CV) experiments were carried out on a CHI 600D electrochemistry workstation (Shanghai CH Instruments, China), connected to a personal computer. All experiments were performed with a conventional three-electrode system. The modified glassy carbon electrode (GCE) as working electrode, a platinum wire as counter electrode and a saturated calomel electrode (SCE) or Ag/AgCl (sat. KCl) as reference electrode. The assembling interface was tracked by scanning electron microscopy (SEM, S-4800, Hitachi, Japan) and cyclic voltammetric. The pH measurements were made with a pH meter (MP 230, Mettler-Toledo Switzerland).

2.3. Fabrication of the proposed biosensor

A glassy carbon electrode (GCE) with 4 mm diameter was firstly polished with 0.3 and 0.05 μm alumina to obtain mirror-like surface, respectively. To remove the physically adsorbed substance, it was rinsed with deionized water and ethanol in ultrasonic bath and dried at room temperature.

Firstly, 1 mg GS and 2 mg CS were dissolved in 1 mL 1% PDDA solution by ultrasonic dispersion, 10 μL of the resulting suspension was coated onto a pretreated GCE surface and dried in the air. Secondly, the electrochemical deposition of Pt–Pd was performed on CS–GS modified GCE to form PtPd–CS–GS nanocomposites in aqueous solution containing 0.5 mM H_2PtCl_6 and 0.5 mM $PdCl_2$. The deposition time was 200 s and the potential was −0.2 V. Subsequently, 6 μL ChOx (1 mg/mL in 0.1 M PBS, pH 7.0) solutions were dropped on the surface of the electrode to construct a cholesterol biosensor (noted as ChOx/PtPd–CS–GS/GCE). Ultimately, the obtained biosensor was stored at 4 °C when not in use. Scheme 1 showed the schematic diagram of the fabrication of the cholesterol biosensor.

3. Results and discussion

3.1. Characterizations

In order to confirm the microstructure and morphology of as-prepared nanomaterials, scanning electron microscopy (SEM) was used to investigate (Fig. 1). The SEM of graphene sheets (GS) dispersed by CS (Fig. 1A) clearly displays a wrinkled paper-like structure with slightly scrolled edges shapes, which is the standard morphology of Graphene sheets. Then the Pt–Pd nanoparticles appear as bright dots, which occupy almost all of the surface of CS–GS with fairly even, ordered, and close-packed distribution in Fig. 1B, forming an interpenetrating network for favorable conduction pathways of electron transfer. The diameter of the formed randomly dot structures vary from tens to hundreds of nanometers. As ChOx was immobilized, a fairly beautiful film was formed like cotton ball (Fig. 1C), providing a good platform for biosensing.

The cyclic voltammetric behavior of the step by step surface modification of the GCE in 5 mM potassium ferricyanide solution (pH 7.0) containing 0.1 M KCl from −0.2 to 0.6 V at a scan rate of 50 mV/s is shown in Fig. 2. The CV wave of bare GCE showed a well defined redox wave in Fig. 2a, corresponding to the reversible redox reaction of ferricyanide ions. The curve b in Fig. 2 was the CV of CS–GS modified GCE. Compared with the bare GCE, the redox wave was obtained at more negative potentials because the positive surface of PDDA modified electrode would attract $Fe(CN)_6^{4-/3-}$ redox couple. When the Pt–Pd nanoparticles were deposited in CS–GS membrane (curve c in Fig. 2), a large peak current was obtained owing to Pt–Pd nanoparticles may act as a bridge of electron transfer and promote the electron transfer. After ChOx was successively loaded onto the electrode surface,

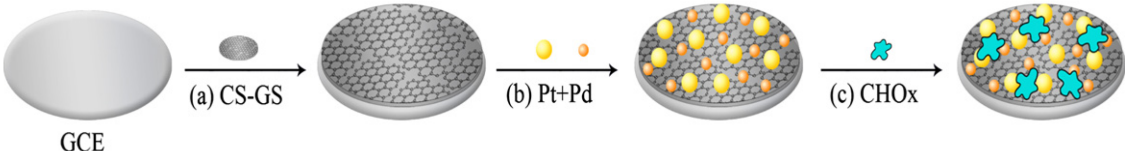

Scheme 1. The schematic diagram of the fabrication of the cholesterol biosensor.

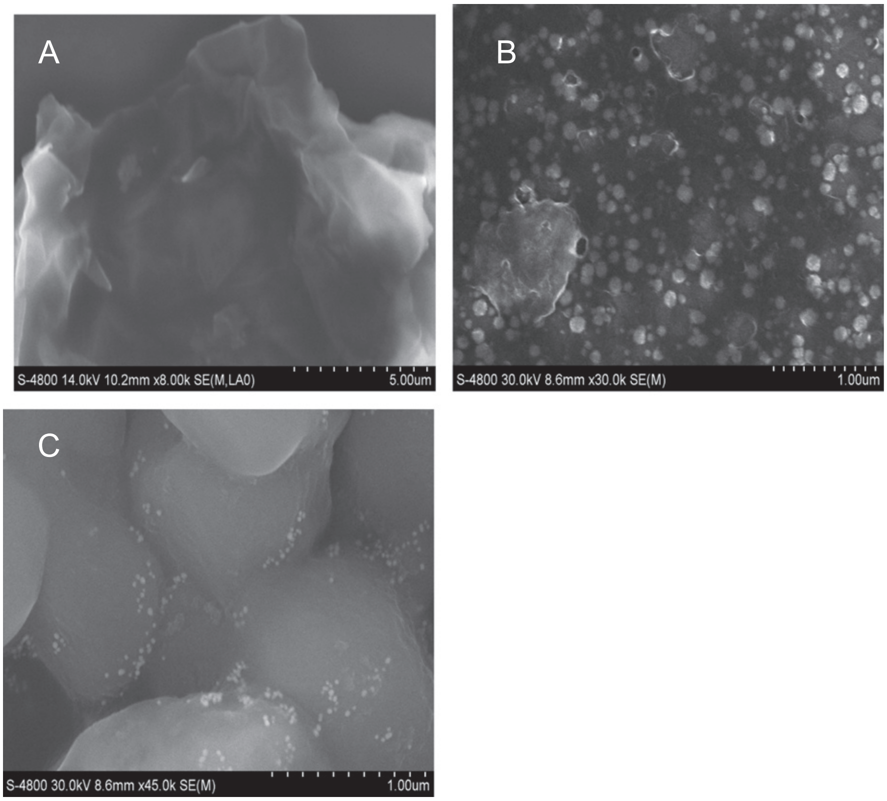

Fig. 1. SEM images of different modified substrates (A) CS–GS, (B) PtPd–CS–GS, (C) ChOx/PtPd–CS–GS.

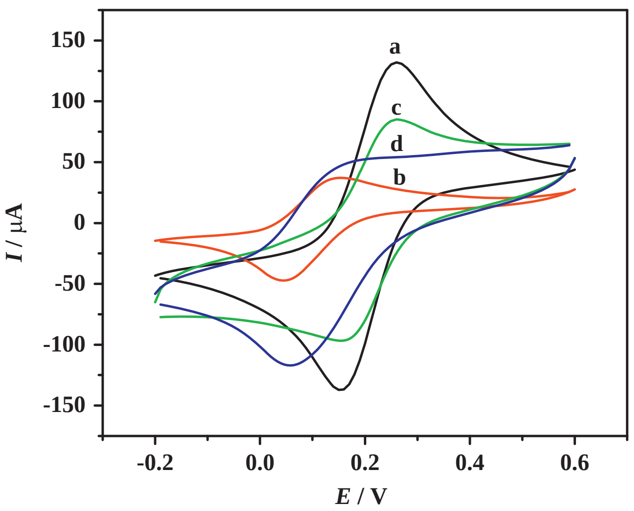

Fig. 2. CVs of different electrodes (a) GCE, (b) CS–GS/GCE, (c) PtPd–CS–GS/GCE, (d) ChOx/PtPd–CS–GS/GCE in 5 mM potassium ferricyanide solution (pH 7.0) containing 0.1 M KCl at 50 mV/s.

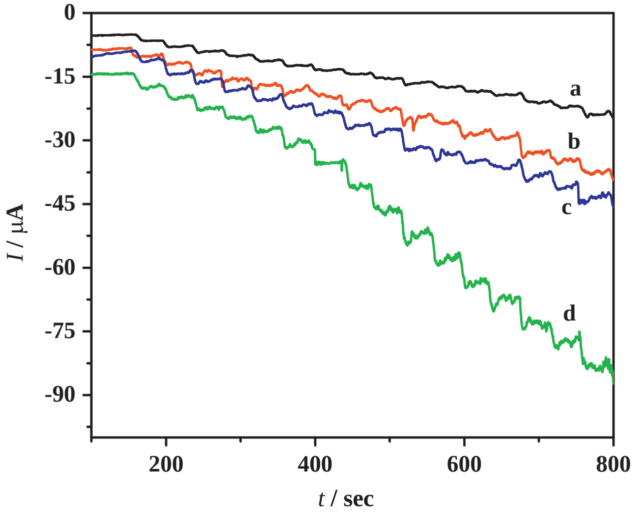

Fig. 3. The amperometric response currents of reduction of H_2O_2 at different electrodes (a) Pd–Au/CS–GS/GCE, (b) Pt–Au/CS–GS/GCE, (c) Pt–Pd–Au/CS–GS/GCE, (d) Pt-Pd/CS–GS/GCE in 5 mL 0.1 M PBS at pH 7.0.

curve d in Fig. 2 shows that the voltammetric response decreases as the formation of a hydrophobic protein layer which insulates the conductive support and the interfacial electron transfer.

3.2. *The comparison of different alloy to signal amplification*

In order to evaluate the effect of different alloy (Pt–Au, Pt–Pd, Au–Pd and Pt–Au–Pd) for the signal amplification, four kinds of different alloy modified GCE electrode were prepared. Fig. 3 presents the amperometric response currents of reduction of H_2O_2 at different electrodes. The GCE modified by CS–GS (CS–GS/GCE) which was covered by electrodeposition of Pd–Au nanoparticles again (Pd–Au/CS–GS/GCE, curve a) showed a worse response compared to the electrodes modified with Pt–Au nanoparticles (Pt–Au/CS–GS/GCE, curve b), Pt–Pd–Au nanoparticles(Pt–Pd–Au/CS–GS/GCE, curve c) and Pt–Pd nanoparticles (Pt–Pd/CS–GS/GCE, curve d). Response current was greatest for modified electrodes with Pt–Pd nanoparticles (Pt–Pd/CS–GS/GCE, curve d). The consequence of the above figure analyses is that, although the different alloy (Pt–Au, Pt–Pd, Au–Pd and Pt–Au–Pd) possessing similar geometric properties (particle size, shape, composition, electrochemical active area) and similar intrinsic kinetic activity (k°), their specific H_2O_2 catalytic activities are different, which were decided by their unique electronic properties. According to the literature [12], the reason may be that Pt–Pd with electron-rich Pt sites could sustain the relatively weak adsorption energy of H_2O_2 and associated reaction intermediates. Therefore, for this Pt–Pd/CS–GS nanocatalyst, facile desorption of surface-bound species and the availability of more $[H_2O_2]_{ads}$/anion-free Pt sites for further continuous H_2O_2 oxidation are expected. So in this study, the electrodes were modified with Pt–Pd nanoparticles (Pt–Pd/CS–GS/GCE) for further experiments prior to adsorption of ChOx.

3.3. Optimization of main experimental conditions

The effect of pH on the performance of the ChOx/PtPd–CS–GS/GCE electrodes was investigated over the pH values from 5.5 to 8.5 in the detection solution containing 0.05 mM cholesterol. As can be seen in Supplementary Fig. 1(A), the current response was found to be maximum at pH 7.0, indicating that the biosensor is more active at this pH and the immobilized ChOx retains its natural structure and does not denature. At higher or lower pHs, enzyme activity is less, which could be due to deactivation/leaching of enzyme from the electrode surface. Thus, all the performance tests of the biosensor were conducted at pH 7.0 to simulate the physiological condition.

Since ChOx catalyzes the aerobic oxidation of cholesterol with concomitant production of H_2O_2, the amperometric response of the ChOx/PtPd–CS–GS/GCE to cholesterol was also investigated in this study. The dependence of the ChOx biosensor response on the applied potential was evaluated over the potential range from −0.5 to 0.0 V for cholesterol in 0.1 M PBS (pH 7.0) (Supplementary Fig. 1(B)). The ChOx/PtPd–CS–GS/GCE electrode showed maximum change in response to a current density of 0.05 mM cholesterol at potential of −0.35 V. Consequently, to investigate further biosensing properties, an operational potential value of −0.35 V was chosen for subsequent amperometric measurements for cholesterol.

3.4. Electrocatalytic activity of ChOx immobilized on the PtPd–CS–GS/GCE electrode

Fig. 4A presents the two CV curves of the ChOx/PtPd–CS–GS/GCE electrode recorded in a phosphate buffer solution (pH 7.0) in the absence of cholesterol (curve a) and in the presence of 0.30 mM cholesterol (curve b). The ChOx/PtPd–CS–GS/GCE electrode showed quasi reversible behaviors, indicating that DET has been achieved between the ChOx and the underlying electrode. Comparison of the two CV curves shows that the addition of cholesterol decreased the anodic current and increased the cathodic current, revealing the strong response of the ChOx/PtPd–CS–GS/GCE electrode to cholesterol.

The current–time amperometric curve is recorded under the conditions of continuous stirring of the solution and successive step changes of cholesterol concentration at −0.35 V (as shown in Fig. 4B). When an aliquot of cholesterol is added into 5 mL 0.1 M PBS at pH 7.0, the reductive current rises steeply to reach a stable value. The time to reach 90% of the maximum current is within 7 s, which indicates a fast response process. The ChOx/PtPd–CS–GS/GCE electrode displays increasing amperometric responses to cholesterol with good linear ranges from 2.2×10^{-6} to 5.2×10^{-4} M with a correlation coefficient of 0.998 (Fig. 4C). The detection limit corresponding to three times the standard deviation of the blank solution was estimated as 0.75 μM. For comparison, the analytical performances of the proposed biosensor were compared with those cholesterol sensors [16–22], as summarized in Table 1, including Michaelis–Menten constant (K_m^{app}), linear range, response time and detection limit. It could be found that the proposed biosensor exhibited satisfactory detection limit and linear range. The reasons might be attributed to the nanocatalyst in the PtPd–CS–GS having a higher

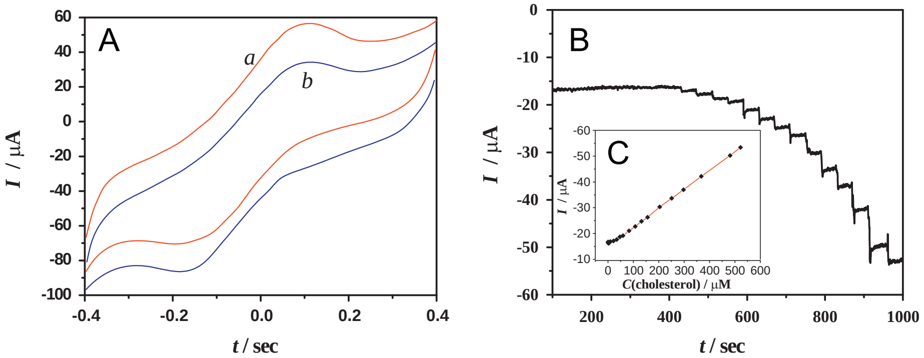

Fig. 4. (A) CVs of the ChOx/PtPd-CS-GS/GCE electrode in 5 mL 0.1 M PBS at pH 7.0 without cholesterol (a) and with 0.30 mM cholesterol (b); (B) The amperometric current–time response for increasing cholesterol concentrations at the biosensor in 5 mL 0.1 M PBS at pH 7.0 and (C) the calibration curve.

Table 1
Comparison of the responses of some cholesterol biosensors constructed based on different modified electrode materials.

Electrode	K_m^{app} /mM	Linear range (M)	Detection limit (M)	Response time/s	References
IL–Ch–AuPt/ChOx	0.24	5.0×10^{-5} to 6.2×10^{-3}, 6.2×10^{-3} to 11.2×10^{-3}	1.0×10^{-5}	< 7	[16]
(MWNTs)–Au/PPD–ChOx	7.17	5.0×10^{-4} to 6.0×10^{-3}	2.0×10^{-4}	30	[17]
PTMSPA–HRP/ChOx–ME	–	1.0×10^{-3} to 2.5×10^{-2}	5.0×10^{-4}	–	[18]
Chit–LDHs/HRP/ChOx	–	4.0×10^{-8} to 6.0×10^{-4}	4.0×10^{-8}	–	[19]
Chit–Hb/Chit–ChOx	–	1.0×10^{-5} to 6.0×10^{-4}	9.5×10^{-6}	50	[20]
Ti/NPAu/ChOx–HRP–ChE	0.64	9.7×10^{-4} to 7.8×10^{-3}	1.3×10^{-5}	Fast	[21]
MWNT(SH)–Au/Chi–IL/ChOx	–	0.5×10^{-3} to 5.0×10^{-3}	–	7	[22]
GS–CS–PtPd/ChOx	0.11	2.2×10^{-6} to 5.2×10^{-4}	7.5×10^{-7}	< 7	This work

electrocatalytic activity, which could enhance the access chance of the ChOx and cholesterol.

The apparent Michaelis–Menten constant (K_m^{app}), which gives an indication of the enzyme–substrate kinetics, can be estimated from the Lineweaver–Burk equation [23]. The K_m^{app} of the prepared ChOx biosensor was calculated to be 0.11 mM, which is much lower than the cholesterol biosensors reported in the literature (Table 1). The small K_m^{app} value indicates that the immobilized enzymes possess high enzymatic activity and that the fabricated biosensor exhibits a high affinity for cholesterol.

3.5. *Reproducibility, stability and anti-interference activity of the biosensor*

Reproducibility and long-term stability are major requirements for a reusable biosensor. The repeatability of the ChOx biosensor was measured in 5 mL 0.1 M PBS at pH 7.0. In a series of seven successive measurements, 0.05 mM cholesterol was measured continuously, and a good repeatability with a relative standard deviation (RSD) of 4.1% was obtained. Reproducibility with respect to the ChOx biosensor was evaluated by the comparison of the currents generated by different electrodes prepared under the same conditions. The amperometric response of seven ChOx/PtPd–CS–GS/GCE electrodes to 0.05 mM cholesterol was examined, the results revealed that the biosensor has satisfactory reproducibility with a RSD of 3.9%.

The long-term stability of the ChOx biosensor was followed by measuring the response to 0.05 mM cholesterol. The biosensor was stored at 4 °C when not in use. The response was found to remain at 96.5% of its original response after 15 days, even after a prolonged storage (35 days), the electrode retained 92.1% of its initial response, indicating good long-term stability. Excellent reproducibility and stability indicated that the catalyst layer on the electrode's surface was structurally stable and free from morphological changes.

To assess the anti-interference capability of the ChOx biosensor, its current–time response to successive additions of 0.1 mM possible interference of ascorbic acid (AA), uric acid (UA), glucose (GL) and 0.05 mM cholesterol was studied in 5 mL 0.1 M PBS (pH 7.0) at a working potential of −0.35 V. The Fig. 5 shows that there was no response to any of the three organic compounds, a strong and fast response was observed only when cholesterol was added, indicating that the biosensor possessed high selectivity for cholesterol. The negligible interference on the current response of enzyme catalysis may be due mainly to the negative working potential.

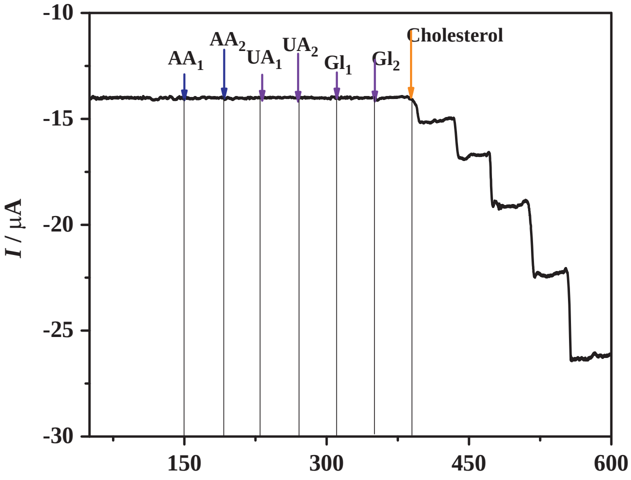

Fig. 5. The amperometric current–time response at the ChOx biosensor toward AA, UA, glucose and cholesterol in 5 mL 0.1 M PBS at pH 7.0.

3.6. *Real sample analysis*

For practical applications, the developed ChOx biosensor was used for the determination of cholesterol in real food samples meat, fish oil, margarine and egg. The real samples were prepared using the same procedure as the cholesterol solution described in Section 2.1, cholesterol concentrations should fall in the working range of above mentioned electrodes. The amount of cholesterol found in meat, fish oil, margarine, and egg was 89.24, 41.28, 0.26 and 380.26 mg/100 g, respectively. This is in good agreement with the amount of the cholesterol listed on the product labels. All these results show that the fabricated cholesterol biosensor offers a great potential of application in cholesterol quality control of food products.

4. Conclusions

The present study demonstrates a new approach toward advanced development of highly sensitive electrochemical assay of cholesterol in food samples by using PtPd–CS–GS hybrid nanocomposites functionalized glassy carbon electrode. Use of the PtPd–CS–GS hybrid nanocomposites not only accelerated direct electron transfer from the redox enzyme to the electrode surface, but also enhanced the immobilized amount of ChOx, greatly improved the electrochemical properties of the biosensor interface. Moreover, the sensitivity of the biosensor could be enhanced greatly. The biosensor also demonstrated excellent stability and resistance to interference. Compared with other works, highlight of this paper is to design an improved enzyme sensing interface in combination with the unique properties of the PtPd–CS–GS hybrid nanocomposites and reveal the specific cholesterol catalytic activity of the biosensor is primarily controlled by the unique electronic properties of the hybrid nanocomposites by way of influencing charge transfer between the electrode and the analyte.

Acknowledgments

This work was supported by National Natural Science Foundation of China (21075100, 21275119), the Ministry of Education of China (Project 708073), the Nature Science Foundation of Chongqing City (CSTC-2011BA7003 and CSTC-2009BA1003) and Specialized Research Fund for the Doctoral Program of Higher Education (20100182110015).

Appendix A. Supplementary Information

Supplementary data associated with this article can be found in the online version at http://dx.doi.org/10.1016/j.talanta.2013.02.002.

References

[1] R. Manjunatha, D.H. Nagaraju, G.S. Suresh, J.S. Melo, S.-F. D'Souza, T.V. Venkatesha, J. Electroanal. Chem. 651 (2011) 24–29.
[2] K.-J. Huang, D.-J. Niu, X. Liu, Z.-W. Wu, Y. Fan, Y.-F. Chang, Y.-Y. Wu, Electrochim. Acta 56 (2011) 2947–2953.
[3] L. Gorton, A. Lindgren, T. Larsson, F.D. Munteanu, T. Ruzgas, I. Gazaryan, Anal. Chim. Acta 400 (1999) 91–108.
[4] Q. Lu, X. Dong, L.-J. Li, X. Hu, Talanta 82 (2010) 1344–1348.
[5] J.J. Feng, G. Zhao, J.J. Xu, H.Y. Chen, Anal. Biochem. 342 (2005) 280–286.

[6] X. Zhao, Z. Mai, X. Kang, X. Zou, Biosens. Bioelectron. 23 (2008) 1032–1038.
[7] R. Jafri, T. Arockiados, N. Rajalakshmi, S. Ramaprabhu, J. Electrochem. Soc. 157 (2010) 874–879.
[8] Q. Zeng, J.-S. Cheng, X.-F. Liu, H.-T. Bai, J.-H. Jiang, Biosens. Bioelectron. 26 (2011) 3456–3463.
[9] C. Zhu, S. Guo, Y. Zhai, S. Dong, Langmuir 26 (2010) 7614–7618.
[10] Y. Wang, R. Yuan, Y. Chai, Y Yuan, L. Bai, Y. Liao, Biosens. Bioelectron. 30 (2011) 61–66.
[11] B. Su, D. Tang, Q. Li, J. Tang, G. Chen, Anal. Chim. Acta 692 (2011) 116–124.
[12] K.-J. Chen, K.C. Pillai, J. Rick, C.-J. Pan, S.-H. Wang, C.-C. Liu, B.-J. Hwang, Biosens. Bioelectron. 33 (2012) 120–127.
[13] K.-J. Chen, C.-F. Lee, J. Rick, S.-H. Wang, C.-C. Liu, B.-J. Hwang, Biosens. Bioelectron. 33 (2012) 75–81.
[14] A. Safavi, F. Farjami, Biosens. Bioelectron. 26 (2011) 2547–2552.
[15] X. Kang, Z. Mai, X. Zou, P. Cai, J. Mo, Anal. Biochem. 369 (2007) 71–79.
[16] A. Safavi, F. Farjami, Biosens. Bioelectron. 26 (2011) 2547–2552.
[17] M. Guo, J. Chen, J. Li, L. Nie, S. Yao, Electroanalysis 16 (2004) 1992–1998.
[18] K.-M. Manesh, P. Santhosh, A.-L. Gopalan, K.-P. Lee, Electroanalysis 22 (2010) 2467–2474.
[19] S.-N. Ding, D. Shan, T. Zhang, Y.-Z. Dou, J. Electroanal. Chem. 659 (2011) 1–5.
[20] C.-Z. Zhao, L. Wan, L. Jiang, Q. Wang, K. Jiao, Anal. Biochem. 383 (2008) 25–30.
[21] A. Ahmadalinezhad, A.-C. Chen, Biosens. Bioelectron. 26 (2011) 4508–4513.
[22] A.- I. Gopalan, K.-P. Lee, D. Ragupathy, Biosens. Bioelectron. 24 (2009) 2211–2217.
[23] R.-A. Kamin, G.-S. Wilson, Anal. Chem. 52 (1980) 1198–1205.